6.4   Padre Cruz Viaduct

6.4.1 Description of structure

The Padre Cruz viaduct is a multi-span bridge in Lisbon with a deck of 32.5m width, maximum spans of 100 m and a total length of approximately 900 m (see Fig. 6-11). This example shows the application of strut-and-tie and stress field models for the design of the main piers of the viaduct for vertical loads. Different levels of approximation analysis are developed to illustrate the application and the differences of each level/approach.

Fig. 6-11 General view after construction (2007)

Fig. 6-12 and Fig. 6-13 show the longitudinal section of the bridge and a transverse section near the support, respectively. The pier section is variable along the height and the section geometry is defined in Fig. 6-14a. The reinforcement layout, presented in Fig. 6-14b was mainly governed by two load combinations: vertical loads and seismic action.

The properties of the materials for the piers were:
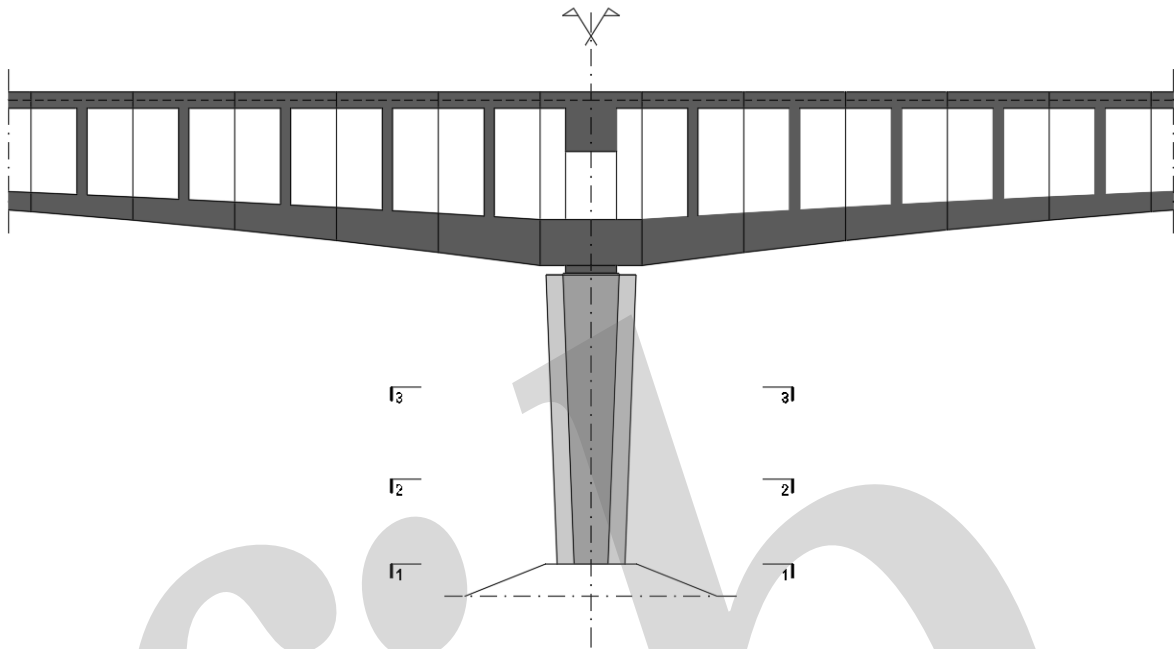
Concrete C40. Steel S500. Prestress Y1860/1670.
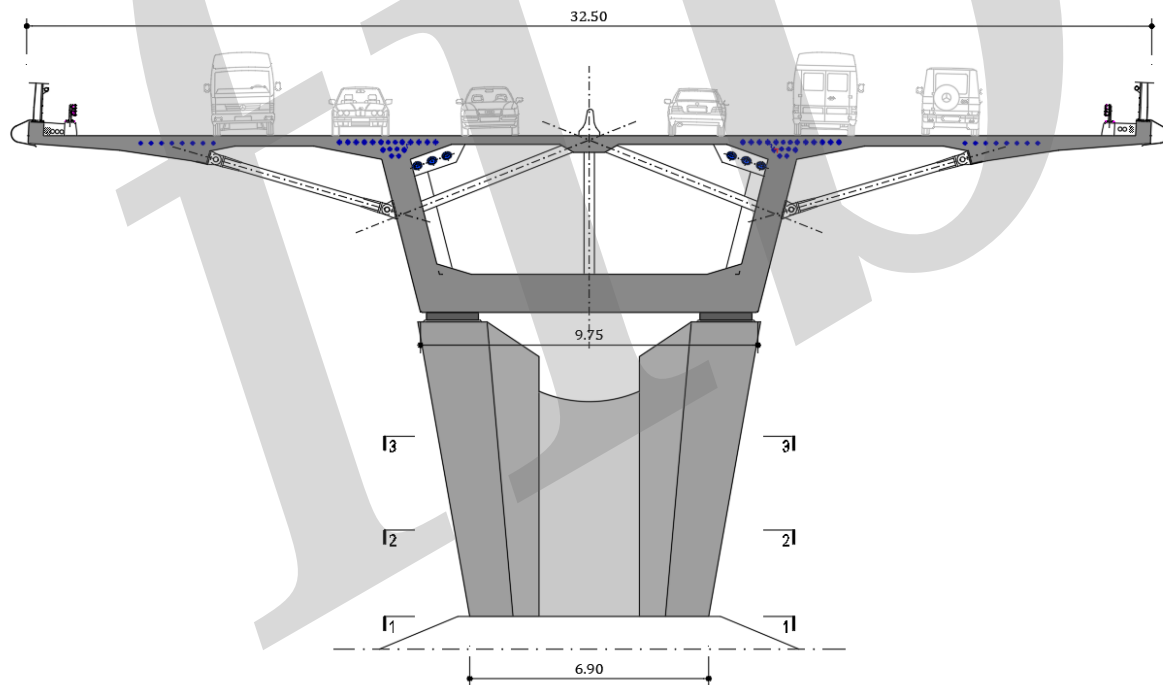
Fig. 6-12 Longitudinal section

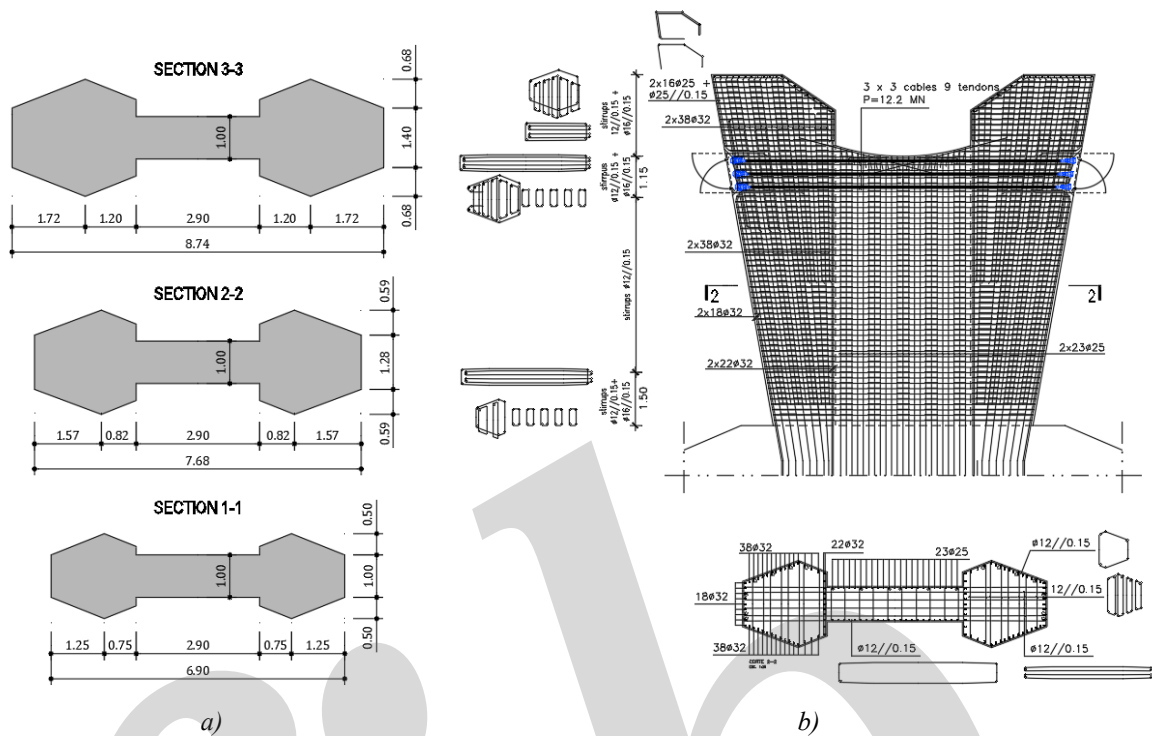Fig. 6-13 Deck section at the supports region and column front view

Fig. 6-14 a) Pier section; b) Reinforcement layout

6.4.2 LoA I Model

The design model presented in this and the next chapter was, in fact, the design model of the pier for the vertical loads at the design stage, however the example is being presented as a check of the already defined reinforcement layout to be extended to the remaining levels of approximation.

The model for the lowest LoA is mainly based on the combination of two simple and basic strut-and-tie models presented in Section 4, even if it looks like a more complex and elaborate model. The model is presented in Fig. 6-15, where the load path defined by model M1 is identical to a common deep beam model with top loads, so the inner level arm z_1 was set to approximately $0.7L_1$. It is easy to observe the similarity of model M2 with a deep beam with suspended loads, though the same ratio between the inner level arm z_2 and the distance L_2 was used. Since the practical rules presented earlier for each basic model were followed, namely the inner level arms of each basic model, ductility and service behaviour topics are automatically checked and no further calculations to check service behaviour are necessary.
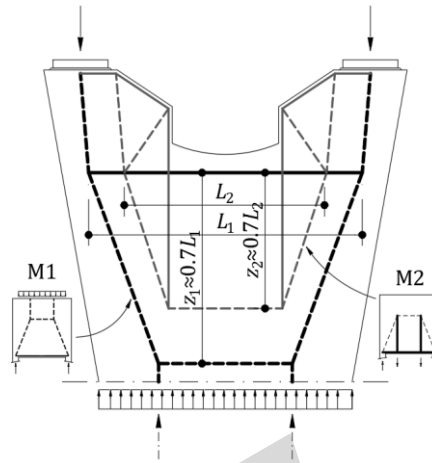
Fig. 6-15 Draft strut-and-tie model based in the combination of two basic models

The resultant model can then be calculated and the forces in the struts and ties are obtained (Fig. 6-16a). The geometry of the model is also presented in Fig. 6-16b.
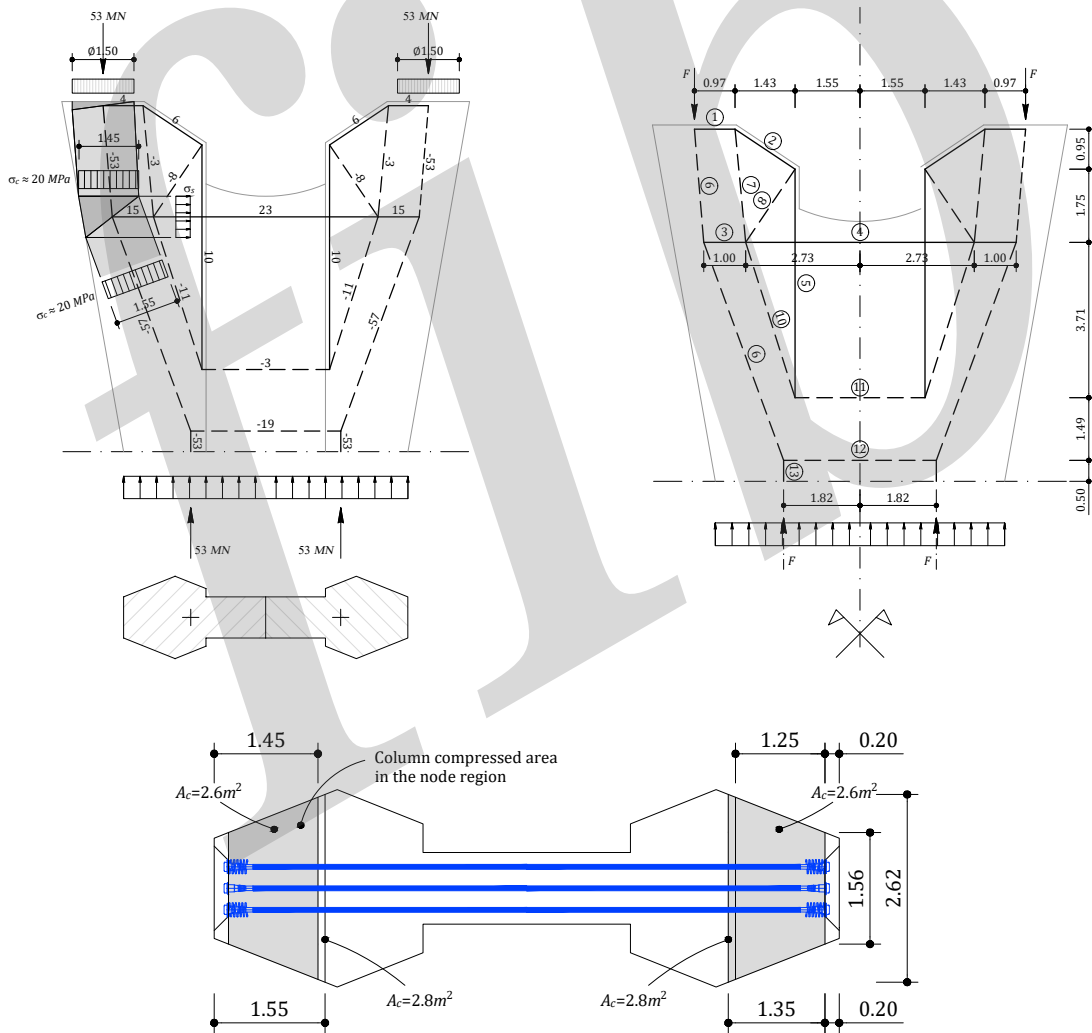

Fig. 6-16 a) Design strut-and-tie model; b) Model geometry and element numbering; c) Plan view of the compressed area.

The inclination of compressive force C_6 (Fig. 6-16b) was defined to limit the compressive stresses at the node region (CCT node of strut 6 and tie 3) to its design strength $\sigma_{c,Rd}$ for a compression-tension node given by 7.3.6.4 of MC2010[6-1]. Note that, the reinforcement is arranged in multiple layers and the angle between the strut and tie is greater than 45°; the design strength may thus be increased by 10% according to 7.3.6.2 of MC2010. The effect of the prestressed plates behind the node provides a state of pure compression, increasing the compressive strength at the node region, but it was not considered, leading to a safe-side design:

$$\sigma_{c,Rd} = 0.75 \cdot \left(\frac{30}{f_{ck}}\right)^{\frac{1}{3}} \cdot f_{cd} \cdot 1.1 = 0.75 \cdot \left(\frac{30}{40}\right)^{\frac{1}{3}} \cdot \frac{40}{1.5} \cdot 1.1 = 20 \text{ Mpa} \qquad 6\text{-}3$$

There is no other critical nodal region, nor high compressive stresses crossing areas of transversal tensile strains, and the check of the pier is, therefore, mainly based on the check of the ties as summarised in Table 6-1.

Table 6-1 Tension and provided reinforcement for LoA I model

Tension	Reinforcement	Steel area	Tensile strength	Check
$T_1 = 4\ MN$	2 × 16Ø25	15'712 mm²	$T_{Rd} = 6.8\ MN$	Ok
$T_2 = 6\ MN$	2 × 16Ø25	15'712 mm²	$T_{Rd} = 6.8\ MN$	Ok
$T_5 = 10\ MN$	2 × 22Ø32	35'376 mm²	$T_{Rd} = 15.4\ MN$	Ok
$T_4 = 23\ MN$	2 × Ø16//0.15 (1.15m) + 4 × Ø12//0.15 (1.15m) + 9c × 9t (150 mm² each tendon)	6'547 mm² + 12'150 mm²	$T_{Rd} = 20.5\ MN$	Not ok

6.4.3 LoA II Model

For the LoA II model for this case a full stress field model was defined as shown in Fig. 6-17. The model considers the provided horizontal web reinforcement in the pier, and in this way, reduces the force in the main tie from 23 *MN* to 20 *MN*. It is a statically-indeterminate model and the tensile force of 3 *MN* was set to a value slightly lower than the yielding force of the provided web reinforcement. The remaining ties have minor and not relevant reductions. With this model it is also possible to check all compressive stresses and check any critical regions, especially if important compressive stresses cross high-tensile strains, which in this case is not relevant, as mentioned before (see Table 6-2). Only the web and main reinforcement must be checked. The remaining are lower than in the previous analysis.

Table 6-2: Tension and provided reinforcement for LoA II model

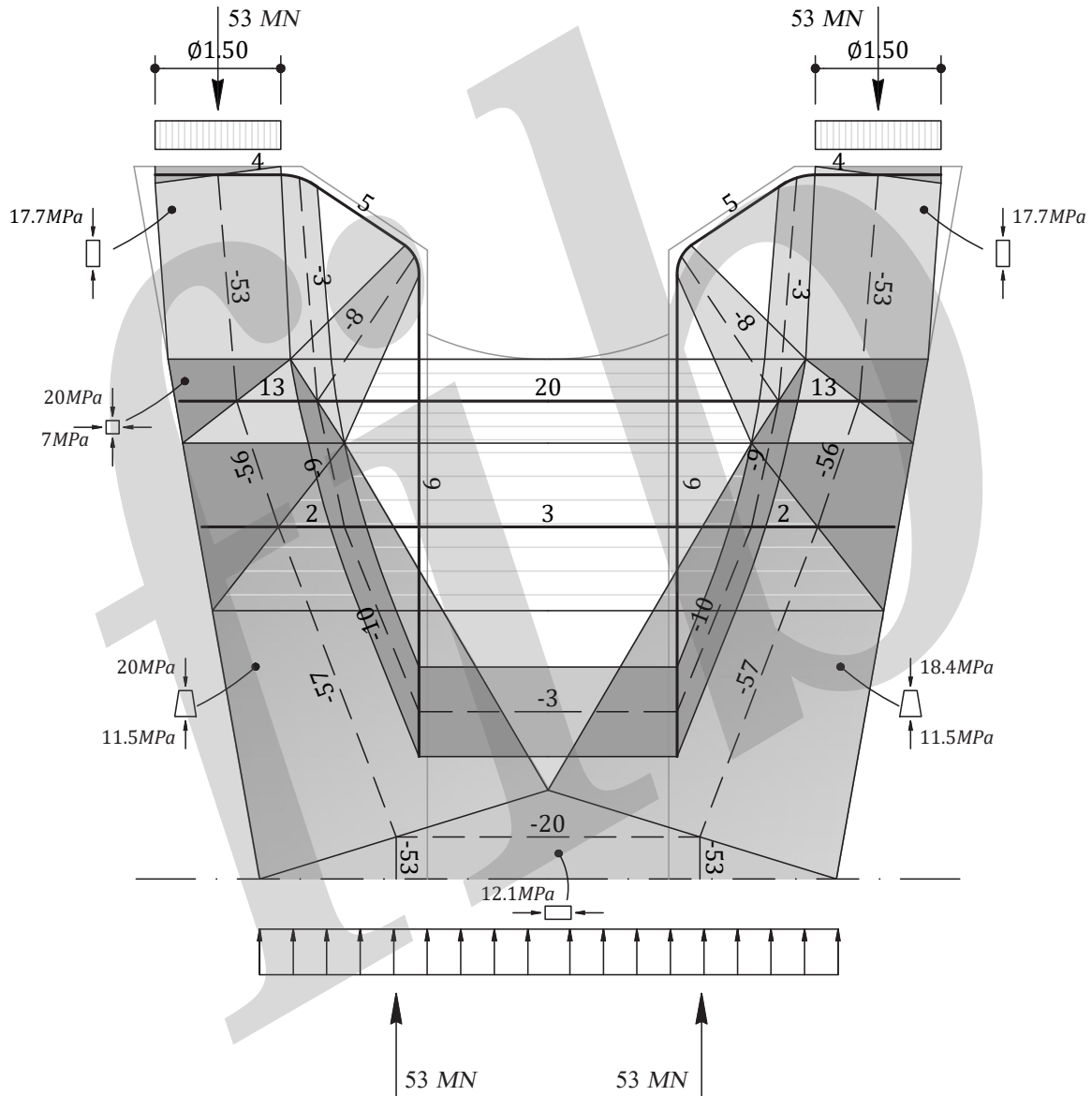| Tension	Reinforcement	Steel area	Tensile strength	Check
$T = 20\ MN$	2 × Ø16//0.15 (1.15m) + 4 × Ø12//0.15 (1.15m) + 9c × 9t	6547 mm^2 + 12150 mm^2	$T_{Rd} = 20.5\ MN$	Ok
$T = 3\ MN$	6 × Ø12//0.15 (2.0 m)	9040 mm^2	$T_{Rd} = 3.9\ MN$	Ok

Fig. 6-17 Pier stress field model for vertical loads

6.4.4 LoA III Model

For this level of approximation, the finite element method is applied. The common parabolic constitutive relationship for the concrete without tensile resistance and an elastic-plastic σ_s-ε_s relationship for the steel is implemented. The compressive stresses in

Practical examples

the concrete and the tensile stresses in the reinforcement are presented in Fig. 6-18. The resultant tensile force in the main tie is less critical than in the previous analyses, with the main reason being the distribution of the vertical reactions at the base of the pier. In the previous LoAs, a uniform distribution of stresses at the base of the piers was assumed, since no compatibility of deformations was provided (see Fig. 6-16 and Fig. 6-17). However, the finite element analysis resulted in a non-uniform stress distribution at the bottom of the pier (see Fig. 6-18c), leading to a steeper inclination of the main compressive force (C_6) and, consequently, to a significant reduction at the main tie force from 20 MN to 14 *MN*. Similarly, the tension in the web reinforcement was also significantly reduced from 3 *MN* to 1.3 *MN*.

This analysis confirmed that concrete compression is not a critical issue and no significant compression softening occurs in regions with high compressive stresses. The only region where a significant reduction of concrete stresses occurs is near the re-entrant corner (see Fig. 6-18d), at the intersection of the vertical tie and main horizontal tie, but no compression crosses that region.
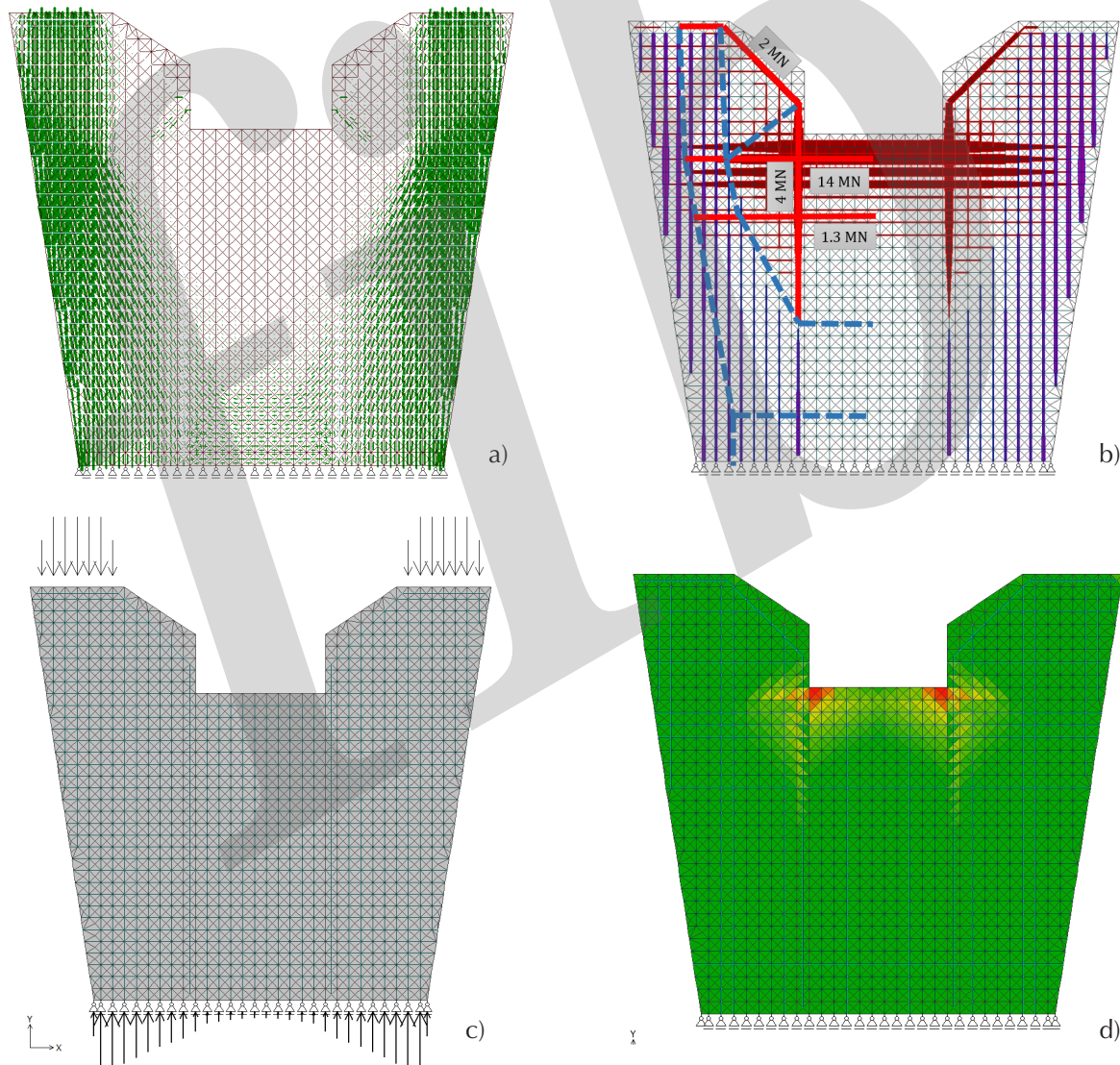

Fig. 6-18 a) Principal compressive stresses b) Reinforcement tensile stresses c) Reactions d) Compression softening

6.4.5 LoA IV Model

For this LoA finite element analysis was also performed, with the addition of a tension stiffening law for the steel. The results at ultimate load are identical to the previous analysis; however, the present analysis allows checking service behaviour, as well. The service load is 40 *MN* for each pot bearing and a prestress of 12.2 *MN* is introduced in the model to properly evaluate the steel stresses and the service behaviour.

Maximum steel stresses of about 170 MPa were obtained, leading to adequate service behaviour (see Fig. 6-19). Even in the absence of any prestressing, steel stresses were as low as 250 MPa, also leading to a satisfactory service behaviour. However, the solution with prestressing provides improved service behaviour and a global increase of the quality of the solution, since steel stresses of low value lead to limited crack width.
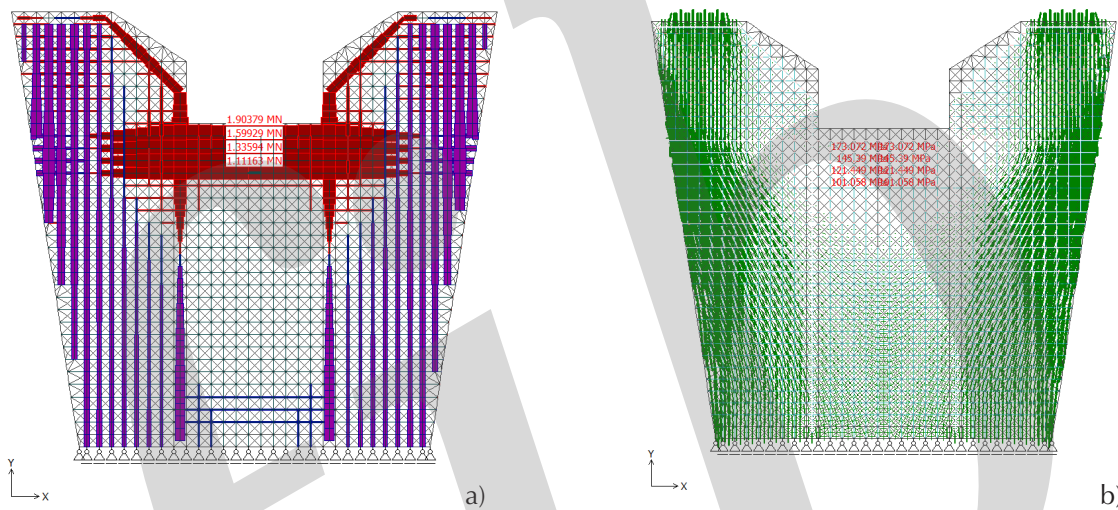

Fig. 6-19 a) Tensile forces for service loads b) Steel stresses for service loads

Practical examples